Continuous Liquid Level Sensor Based on Coupled Light Diffusing Fibers

Pasquale Imperatore, *Member, IEEE*, Gianluca Persichetti, Genni Testa, and Romeo Bernini, *Member, IEEE*

***Abstract*—A continuous liquid level fiber optic sensor has been devised, developed, and tested. The sensor is based on two coupled light-diffusing glass fibers. The light from a laser diode is diffused out from the first fiber by scattering and coupled, always by the scattering, to the second fiber. The working wavelength has been selected in order to be strongly absorbed by most common liquids. The optical power measured at the ends of the collection fiber depends on liquid level. Both co-propagation and counter-propagation coupling configurations have been theoretically analysed and experimentally tested. Differently from counter-propagation configuration, co-propagation configuration exhibits a linear response with the liquid level and allows level measurements with a resolution in the order of millimetres over 1 m range.**

***Index Terms*—Optical fiber sensors, Liquid level measurement, Light Diffusing Fiber, Power-coupling, Light scattering.**

I. Introduction

LIQUID level sensors play a very important function in several industrial and commercial applications ranging from transportation to chemical plants and environmental monitoring [1]. In particular, level measurements in flammable and explosive environments such as fuel tanks, petrochemical, pharmaceutical, landfill and sewage treatment sites require intrinsically safe sensors that pose complex technical challenges. In these critical applications, conventional level sensors based on electrical devices require a very careful design in order to avoid the risk of spark ignited explosions [2]. In general, the adoption of additional insulation layers and protections is required, with an increase in the complexity and cost of the sensor. For this reason, in recent years, optical fiber technologies for sensing the level of liquids have been widely proposed and tested. In addition to traditional advantages like lightweight, small size and immunity to the electromagnetic interference, the absence of electrical components in the sensing region makes optical fibers a promising technology for the development of intrinsically safe sensors, with application in explosive or hazardous environments.

Manuscript received August 24, 2019; revised December 19, 2019; accepted April 8, 2020. Date of publication April 22, 2020; date of current version June 9, 2020. This work was supported in part by the project IAMICA (I High Technology Infrastructure for Environmental and Climate Monitoring—PONa3_00363). *(Corresponding author: Romeo Bernini.)*

The authors are with the Institute for Electromagnetic Sensing of the Environment, National Research Council of Italy, Napoli, Italy (e-mail: imperatore.p@irea.cnr.it; persichetti.g@irea.cnr.it; testa.g@irea.cnr.it; bernini.r@irea.cnr.it).

Color versions of one or more of the figures in this article are available online at https://ieeexplore.ieee.org.

Digital Object Identifier 10.1109/JSTQE.2020.2988603

Several level point sensors based on Fiber Bragg Grating (FBG) [3] or Long Period Fiber Grating (LPG) sensors [4], have been developed. Other point sensors, based on total internal reflection (TIR) have been widely proposed. Typically, these sensors require specific geometric design in order for TIR occurs, like small prisms or hemi ellipsoidal optic mounted at the end of the fiber [5], [6]. Moreover, conically shaped [7] or angled and retroreflecting-type optical fiber tips [8], [9] have been proposed; however, they are very fragile.

Point sensors are primarily designed for discrete level measurements, e.g., to sense whether the vessel is empty or full or at some intermediate point. If continuous level measurements are required, a multiplicity of such point sensors is needed and the accuracy of measurements is strictly related to the sensor number. Such an approach could imply a complex configuration when high-resolution continuous level monitoring is required. In fact, the assembly and interrogation of hundreds of closely spaced sensors is complex, and it could require sophisticated multiplexed interrogation techniques [6]. Continuous fiber optic sensors have been developed in order to avoid these problems. Interferometric sensors based on a fiber grating, Mach–Zehnder interferometer, Fabry-Perot or on multi modal interference (MMI) have been proposed [10]–[15]. As a matter of fact, these level sensors show very high sensitivity; however, complex measuring systems are typically required.

Intensity-modulated sensors could represent a possible solution, in order to reach large measurement range with high sensitivity. Several approaches based on the measurement of the intensity of light transmitted through an optical fiber with its cladding removed (totally or partially) have also reported [16]–[18]. More recently, macrobend side coupling effect has been used for developing several sensors based on polymer optical fibers [19]–[21]. The performances of several continuous optical level sensors are summarised in Table I.

In this paper, for the first time a sensors based on *coupled light diffusing fibers* (LDF) for continuous measurement of liquid level is proposed. In glass-based LDF, light-scattering centres with submicron size are placed in the core of the fiber [22]. These scattering centres efficiently provide a very uniform scattering of the propagating light through the sides and along the length of the optical fiber. Typically, this kind of fiber has been used for lighting or light delivery in biomedical applications [22], [23]. The sensor consists of two parallel LDFs coupled together. The illuminating fiber is connected to a laser diode and diffuses the light into the liquid. A portion of the light is coupled into the second fiber and delivered to a photodetector. By

TABLE I
CONTINUOUS LEVEL SENSORS CHARACTERISTICS

Sensing principle	Range[m]	Resolution[mm]	Ref
Etched FBG	0.02	2	[10]
Multi-modal interference	0.045	0.46	[13]
Mach–Zehnder interferometer	0.075	15	[14]
Fabry-Perot Interferometer	1	3	[15]
Side-polished fiber	0.04	2.2	[16]
Removed cladding fiber	1	25	[17]
Etched D-shaped fiber	0.02	1	[18]
Macro-bend fiber coupler	0.6	0.008	[21]

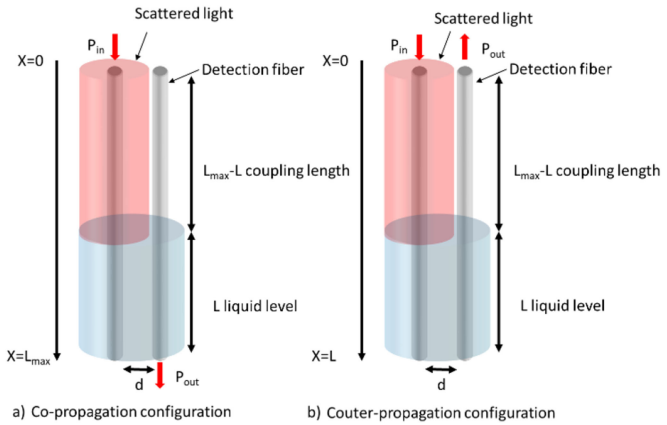

Fig. 1. Schematic layout of the sensor: a) co-propagation configuration, and b) counter-propagation configuration.

choosing a working wavelength strongly absorbed by the liquid, the length of the coupling between the fibers depends on the portion of fiber immersed in the liquid. The coupling phenomena has analytically been modelled by means of *coupled power equations*, and both co-propagation and counter-propagation coupling configurations have been analysed. The variations of output power in co-propagation configuration turn out to be linearly related to the liquid level. The use of the scattering as a coupling mechanism allows to couple the optical fibers, which are however at a relatively large distance in terms of wavelength. Our approach strongly simplifies the sensors fabrication and increases the overall reliability of the sensor. The experimental results are in good agreement with the theoretical model, thus demonstrating the effectiveness of the sensor.

II. LIGHT-COUPLING BASED SENSING PRINCIPLE

In this Section, we qualitatively describe the structure and the physical principle underpinning the behaviour of the proposed sensor, which relies on a light-coupling system employing light-diffusing optical fibers.

The proposed sensor layout is illustrated in Fig. 1. Two parallel light-diffusing fibers are placed side by side at a distance $d \gg \lambda$, where λ is the operating wavelength. The *illuminating* fiber is connected to a light source; the *detection* fiber is linked to the detection system. As a matter of fact, the coupling mechanism implemented relies on scattering form random imperfections in the employed light-diffusing optical fiber, thereby producing a power exchange between the two fibers. Accordingly, the light scattered by the *illuminating* fiber is then coupled, always by the scattering, to the detection fiber. The coupling between the two fibers depends on the properties of the diffusing fiber, the distance d, and the optical properties of the medium between the fibers. Assuming that the liquid strongly absorbs the scattered power, the amount of coupling depends on the length of the fiber portion which is immersed into the liquid. Therefore, the optical power collected by the detection fiber is related to the actual liquid level to be sensed.

The coupling acts along the coupling region $C = \{\mathrm{x} : 0 < x < \mathrm{L}_{max} - \mathrm{L}\}$, where L is liquid level and L_{max} is the range of the sensor (see Fig. 1). Conversely, along the filled-up region $F = \{\mathrm{x} : \mathrm{L}_{max} - \mathrm{L} < x < \mathrm{L}_{max}\}$ no coupling is assumed between the two fibers, since the liquid is strongly absorbent at the working wavelength λ.

According to our framework, both co-propagating and counter-propagating configurations have been considered, as depicted in Fig. 1. A quantitative description of the key light-coupling mechanism employed by the sensor can be given according to the analytical model described in next Section.

III. THEORETICAL MODELLING

Modelling the coupling between the two multimode fibers, which in our configuration is caused by random imperfections of the fibers themselves, is crucial for describing the exchange of power between them. A rigorous description of the coupling among the modes of two multimode optical fibers should involves the classical coupled wave theory and cumbersome derivations [24]. However, because in our configuration the coupling between the fibers is caused by random imperfections of the fibers, the power exchange can be modelled as the coupling between two multimode fibers coupled by a random coupling function. Indeed, this interaction can be more easily described by coupled power equations [25] instead of the classical coupled wave theory, which involves both phase and amplitude of all the modes at any point along the fiber.

As a matter of fact, coupled power equations have commonly been employed for describing the effect of modes coupling in a single optical fiber or between multiple fibers, due to imperfections of the fiber structure [25]–[28]. The analytical derivation of the coupled power equations has been carried out by several authors, with the help of perturbation theory and statistical methods. We remark that, since the available solutions are given only under certain restricting assumptions, we (re)derive the solution of the *coupled power equations* in a general form that is appropriate for our purposes.

A. Co-Propagation Coupling Model

The power coupling between two co-propagating coupling wave can formally be described in terms of a first-order system of ordinary differential equations [24]–[27], in the form:

$$\begin{cases} \frac{\mathrm{dP_0}}{\mathrm{dx}} = -(\alpha+\beta)\,\mathrm{P_0} + \beta \mathrm{P_1} \\ \frac{\mathrm{dP_1}}{\mathrm{dx}} = \quad \beta \mathrm{P_0} - (\alpha+\beta)\,\mathrm{P_1} \end{cases} \tag{1}$$

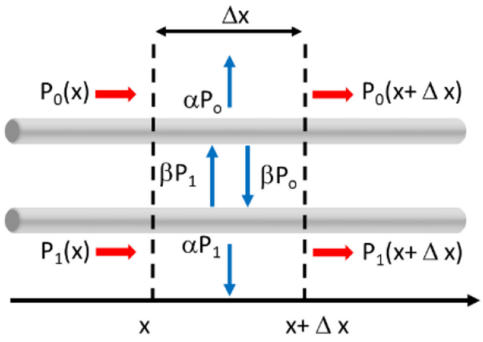

Fig. 2. Co-propagation coupling model: Power balance across an elementary cell of length Δx.

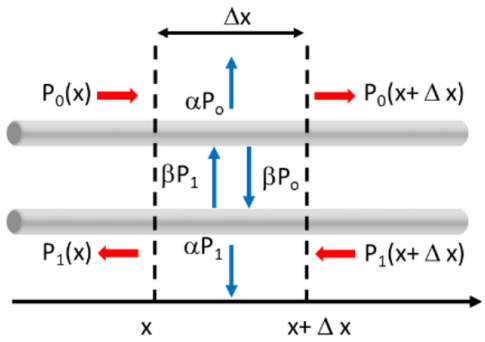

Fig. 3. Counter-propagation coupling model: Power balance across an elementary cell of length Δx.

where $\mathrm{P}_0(\mathrm{x})$ and $\mathrm{P}_1(\mathrm{x})$ describe the average power in the illuminating and detection fiber, respectively; x is the distance along the guide; β is the *coupling coefficient*; α is the (power) attenuation coefficient of fibers. For the sake of simplicity, we assumed equal attenuation in illuminating and detection fibers.

Equation system (1) has a simple intuitive meaning. An interpretation of the finite-difference equation equivalent to (1), in terms of power balance across an elementary cell of length Δx, is provided in Fig. 2.

Due to the liquid absorption $\beta(\mathrm{x})$ can be expressed as:

$$\beta\left(\mathrm{x}\right)=\begin{cases}\beta & 0<x<\mathrm{L}_{max}-L\\ 0 & \mathrm{L}_{max}-L<x<\mathrm{L}_{max}\end{cases} \tag{2}$$

The system (1) applies only to the coupling region $C=\{\mathrm{x}\,:\,0<x<\mathrm{L}_{max}-\mathrm{L}\}$, where L is liquid level and L_{max} is the range of the sensor.

In the co-propagation configuration, the input power P_{in} is injected in the illuminating fiber at $\mathrm{x}=0$, and the output power $\mathrm{P}_{\mathrm{out}}$ is measured at $\mathrm{x}=\mathrm{L}_{max}$ of the detection fiber (see Fig. 1). Accordingly, by imposing the boundary conditions $\mathrm{P}_0(0)=\mathrm{P}_{\mathrm{in}}$ and $\mathrm{P}_1(0)=0$, the inherent solution of system (1) can be expressed in the closed-form:

$$\begin{cases}\mathrm{P}_0\left(\mathrm{x}\right)=\frac{\mathrm{P}_{\mathrm{in}}}{2}\mathrm{e}^{-\alpha\mathrm{x}}\left(1+\mathrm{e}^{-2\beta\mathrm{x}}\right)\\ \mathrm{P}_1\left(\mathrm{x}\right)=\frac{\mathrm{P}_{\mathrm{in}}}{2}\mathrm{e}^{-\alpha\mathrm{x}}\left(1-\mathrm{e}^{-2\beta\mathrm{x}}\right)\end{cases} \tag{3}$$

By using (3), the average-power in the detection fiber evaluated at the end of the coupling length ($\mathrm{x}=\mathrm{L}_{max}-\mathrm{L}$) can be written as $\mathrm{P}_1(\mathrm{L}_{max}-\mathrm{L})=\frac{\mathrm{P}_{\mathrm{in}}}{2}\mathrm{e}^{-\alpha(\mathrm{L}_{max}-\mathrm{L})}(1-\mathrm{e}^{-2\beta(\mathrm{L}_{max}-\mathrm{L})})$. As a result, the (average) output power, i.e., the powered measured at the end of the detection fiber ($\mathrm{x}=\mathrm{L}$), can be expressed as (see also Fig. 1.a):

$$\begin{aligned}\mathrm{P}_{\mathrm{out}}&=\mathrm{P}_1\left(\mathrm{L}_{max}-\mathrm{L}\right)\mathrm{e}^{-\alpha\mathrm{L}}\\&=\frac{\mathrm{P}_{\mathrm{in}}}{2}\mathrm{e}^{-\alpha\mathrm{L}_{max}}\left(1-\mathrm{e}^{-2\beta(\mathrm{L}_{max}-\mathrm{L})}\right)\end{aligned} \tag{4}$$

It should be noted that in the region $F=\{\mathrm{x}\,:\,\mathrm{L}_{max}-\mathrm{L}<x<\mathrm{L}_{max}\}$, the system (1) applies with $\beta=0$ (strongly absorbent liquid), thus justifying the factor $\mathrm{e}^{-\alpha\mathrm{L}}$ appearing in (4).

B. Counter-Propagation Coupling Model

Similarly, the counter-propagating coupling problem can be described in terms of the following first-order system of ordinary differential equations, as follows:

$$\begin{cases}\frac{\mathrm{dP}_0}{\mathrm{dx}}=-\left(\alpha+\beta\right)\mathrm{P}_0+\beta\mathrm{P}_1\\ \frac{\mathrm{dP}_1}{\mathrm{dx}}=-\beta\mathrm{P}_0+\left(\alpha+\beta\right)\mathrm{P}_1\end{cases} \tag{5}$$

These coupled power equations for waves traveling in opposite directions have likewise a simple intuitive meaning and interpretation (see Fig. 3).

The system (5) equally applies to the coupling region C. In the counter-propagating configuration the input power P_{in} is injected in the illuminating fiber at $\mathrm{x}=0$, and the output power $\mathrm{P}_{\mathrm{out}}$ is measured at $\mathrm{x}=0$ of the detection fiber (Fig. 1.b). Therefore, by enforcing the boundary conditions $\mathrm{P}_0(0)=\mathrm{P}_{\mathrm{in}}$ and $\mathrm{P}_1(\mathrm{L}_{max}-\mathrm{L})=0$, we obtain the analytical solution (6) of the equation system (5) in terms of hyperbolic functions. It is reported at the end of this page.

By using (6), we can evaluate the output power, i.e., the power in the detection fiber measured at the end of the coupling length ($\mathrm{x}=0$), as $\mathrm{P}_{\mathrm{out}}=\mathrm{P}_1(0)$ (see also Fig. 1.b). Accordingly, we get the following closed-form expression:

$$\begin{cases}\mathrm{P}_0\left(\mathrm{x}\right)=\mathrm{P}_{\mathrm{in}}\cosh\left(\sqrt{\alpha\left(\alpha+2\beta\right)}\mathrm{x}\right)\\ +\frac{\beta\overline{P_1}-(\alpha+\beta)\mathrm{P}_{\mathrm{in}}}{\sqrt{\alpha(\alpha+2\beta)}}\sinh\left(\sqrt{\alpha\left(\alpha+2\beta\right)}\mathrm{x}\right)\\ \mathrm{P}_1\left(\mathrm{x}\right)=\overline{P_1}\cosh\left(\sqrt{\alpha\left(\alpha+2\beta\right)}\mathrm{x}\right)\\ +\frac{(\alpha+\beta)\overline{P_1}-\beta\mathrm{P}_{\mathrm{in}}}{\sqrt{\alpha(\alpha+2\beta)}}\sinh\left(\sqrt{\alpha\left(\alpha+2\beta\right)}\mathrm{x}\right)\end{cases} \tag{6}$$

where $\overline{P_1}=\frac{\mathrm{P}_{\mathrm{in}}\beta}{(\alpha+\beta)+\sqrt{\alpha(\alpha+2\beta)}\coth[\sqrt{\alpha(\alpha+2\beta)}(\mathrm{L}_{max}-\mathrm{L})]}$

$$\mathrm{P}_{\mathrm{out}}=\frac{\mathrm{P}_{\mathrm{in}}\beta}{\left(\alpha+\beta\right)+\sqrt{\alpha\left(\alpha+2\beta\right)}\coth\left[\sqrt{\alpha\left(\alpha+2\beta\right)}\left(\mathrm{L}_{max}-\mathrm{L}\right)\right]} \tag{7}$$

where $\coth[\cdot]$ denotes the hyperbolic cotangent function. Finally, it can easily be verified that the expressions of the obtained solution reduce to those reported in [27], which are valid in the special case of zero attenuation ($\alpha=0$).

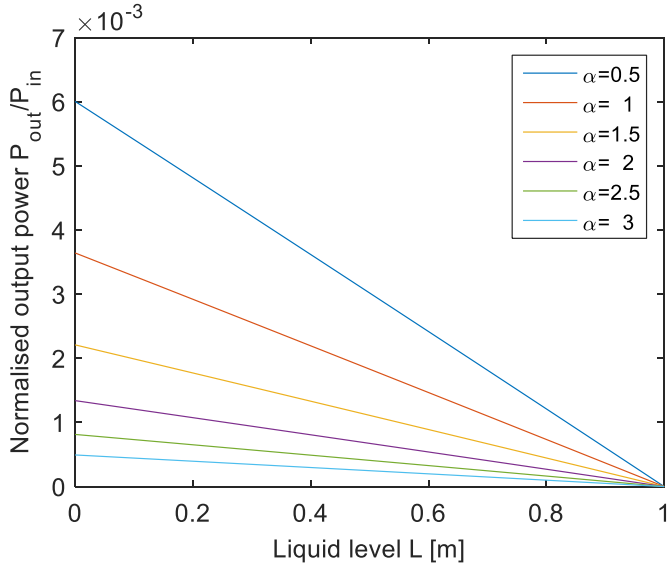

Fig. 4. Co-propagating configuration: Normalised output power P_{out}/P_{in} as a function of the liquid level L, for $\beta = 0.01\,m^{-1}$, $L_{max} = 1$ m, and α ranging from 0.5 to 3 m^{-1}.

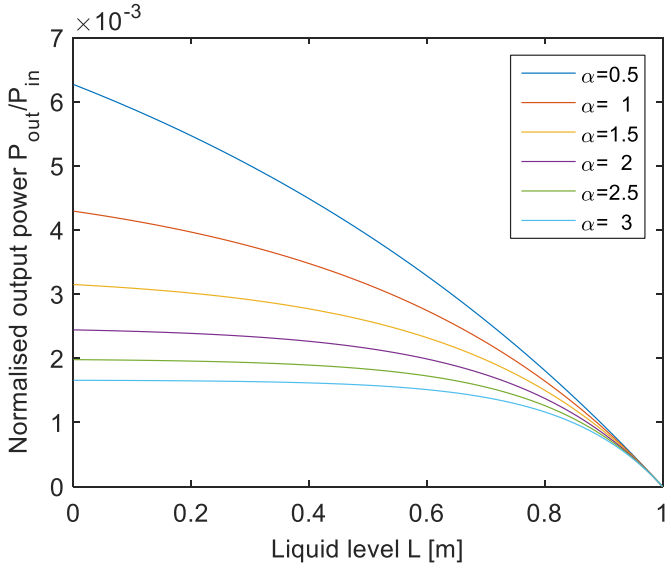

Fig. 5. Counter-propagating configuration: Normalised output power P_{out}/P_{in} as a function of the liquid level L, for $\beta = 0.01\,m^{-1}$, $L_{max} = 1$ m, and α ranging from 0.5 to 3 m^{-1}.

C. Model Parameters and Discussion

In this Section, the derived expressions of the analytical model are specialized with reference to typical parameter values for the considered sensing arrangement, for both co-propagating and counter-propagating configurations. Therefore, the above-mentioned formal solutions are evaluated numerically. The fiber attenuation coefficient α includes both absorption and scattering losses in each fiber. However, in light diffusing fiber the absorption losses are negligible compared to the scattering losses. Considering that the scattering losses in these fibers can be as high as 5-7 dB/m [22], high values of α should be considered. As for β, since the power is emitted by the illuminating fiber over a very large solid angle and $d \gg \lambda$, only a small part of the emitted light is coupled to the detection fiber. Therefore, in the specific sensor arrangement we have considered, a weak-coupling ($\beta \ll 1\ m^{-1}$) regime is expected. The normalised output power P_{out}/P_{in} ($P_{out} = P_{out}\,(L)$) evaluated according to (4) is depicted in Fig. 4 as a function of the liquid level L,, for $\beta = 0.01$ m^{-1}, $L_{max} = 1$ m, and different values of α ranging from 0.5 to 3 m^{-1}. As it can be observed, in the co-propagating configuration the output power is linearly related to the liquid level regardless of the fiber attenuation. This due to fact that, for $\beta \ll 1$, the expression (4) can be approximated as:

$$P_{out} \approx P_{in} e^{-\alpha L_{max}} \beta\,(L_{max} - L) \tag{8}$$

Second, the counter-propagating configuration is concerned. In Fig. 5, the normalise output power evaluated according to (7) is depicted as a function of the liquid level, for $\beta = 0.01\,m^{-1}$, $L_{max} = 1$ m, and different values of α ranging from 0.5 to 3 m^{-1}. Evidently, in this case the output power is nonlinearly related to the liquid level. Notice that the nonlinear behaviour is more pronounced as the α attenuation coefficient increases.

IV. Sensor Fabrication and Experimental Setup

The sensor has been assembled using two light diffusing fibers Fibrance by Corning. Fibrance is a glass fiber which emits 360° uniformly light around the circumference of the fiber and >120° along the length of the fiber, thus acting as a long and flexible cylindrical diffuser [29], [30].

This light diffusing fiber has a silica core in which a section of the core contains a ring of non-periodically distributed (radially and axially) scattering sights. Scattering sights have diameters in the range of$\sim$ 50–500 nm and lengths of $\sim$ 10–1000 mm [22]. Consequently, they effectively scatter the propagating light almost independently of the working wavelength. The amount of scattered light may be controlled, as it depends on the size of the scattering centres and their relative area compared to the fiber core. By tuning the manufacturing process, different diffusion lengths, defined as the length of fiber required to lose ninety percent of the light, can be obtained. Absorption losses within the fiber are negligible, and scattering losses can be as high as 5 -7 dB/m. The bending losses are also weak with minimum bending diameters of 5 mm radius.

Two Fibrance fibers with a diffusion length of 1m have been used in this work. The fiber has a core diameter of 170 $\pm$ 3 μm and a low refractive index polymeric cladding with a diameter of 230 $\pm$ 10 μm [29]. The fiber is protected by a loose tube Polyvinyl chloride (PVC) jacket with an outer diameter of 900 μm. PVC is resistant to many alcohols, fats, oils and aromatic free petrol. It is also resistant to most common corrosive agents, including inorganic acids, alkalis and salts. The properties of the fiber are summarized in Table II.

The sensor is manufactured by a polymeric beam of PVC (1500 × 40 × 5mm), on which the two fibers have been glued side by side at a distance d = 1.5 mm. In order to control and simplify the assembly procedure, the fiber are placed in two U-grooves, 1 × 0.3 mm, machined by micromilling. Two different

TABLE II
LIGHT-DIFFUSING FIBER CHARACTERISTICS

Parameter	Value
Diffusion length	1.0[m]
Numerical aperture	0.5
Core diameter	170 ± 3 [μm]
Cladding diameter	230 ± 10 [μm]
Jacket diameter	900 [μm]

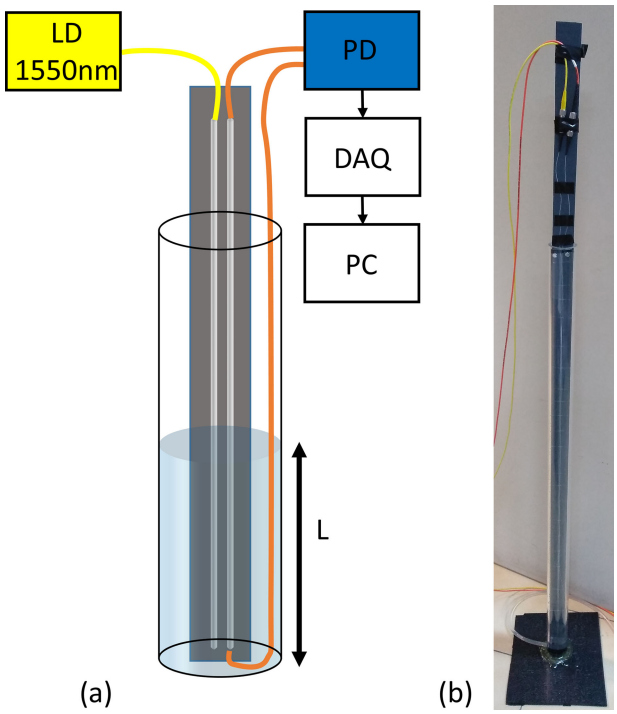

Fig. 6. (a) Experimental setup scheme and (b) photograph of the assembled continuous liquid-level sensor.

sensors for co-propagating and counter-propagating coupling configurations have been assembled.

The experimental setup scheme and a picture of the assembled liquid level sensor are shown in Fig. 6. The sensor is fixed inside a graduated cylindrical testing container and the liquid level ranges from 0 mm to 950 mm continuously by means of a peristaltic pump. A 1550nm fiber coupled laser diode (LD) is employed as light source, with an output power of 30 mW. A high sensitivity photoreceiver (PD) (Thorlabs PDF10C, NEP = 7.5 fW/$\sqrt{}$Hz and a bandwidth of 25Hz) with a data acquisition module (DAQ) connected to a personal computer (PC) is used for measuring the output power of the detection fiber at different liquid levels. The choice of a 25 Hz bandwidth in our tests is motivated by the fact that the proposed sensors is mainly intended for aeronautical applications where fast responses are required. Water has been selected as the test liquid ($\alpha = 1210$ m^{-1} at 1550nm [31]), and all the experiments are conducted by shielding the sensor from ambient light using a black curtain. The fiber attenuation at 1550nm has been evaluated using cut-back technique, resulting in the estimated value $\alpha \approx 1$ m^{-1}. The main characteristics of the employed fiber are summarize in Table II.

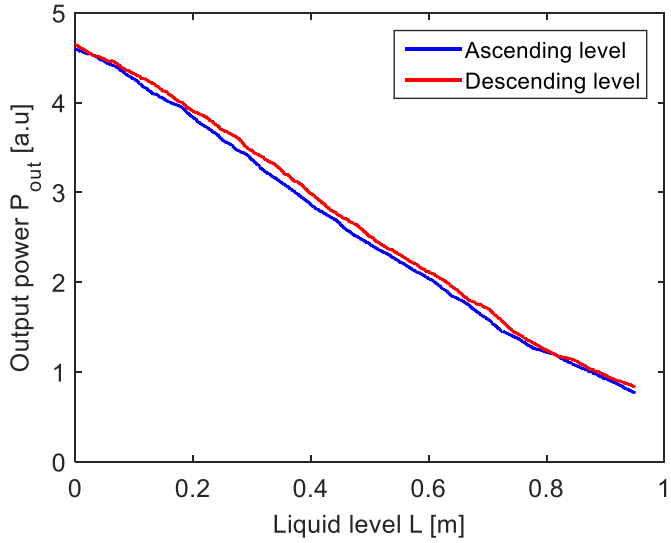

Fig. 7. Co-propagation configuration: Sensor response as a function of the liquid level, for both increasing and decreasing liquid levels, from 0 to 950 mm.

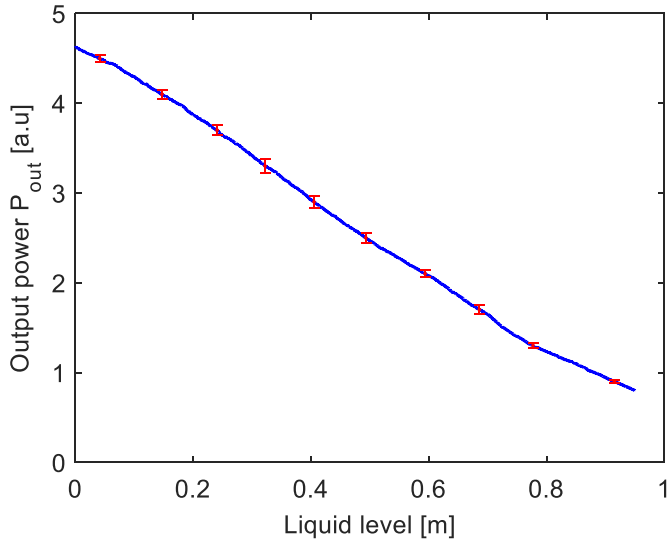

Fig. 8. Co-propagation configuration: Average sensor response as a function of the liquid level; Error bars are also depicted.

V. RESULTS AND DISCUSSION

The performances of the sensor have been assessed by both increasing and decreasing the liquid level from 0 mm to 950 mm. Each test has been repeated 7 times for statistical error analysis.

A. Co-Propagation Configuration

The measured response of the proposed liquid level sensor is shown in Fig. 7. Remarkably, when the liquid level changes from 0 to 950 mm, the output power decreases linearly.

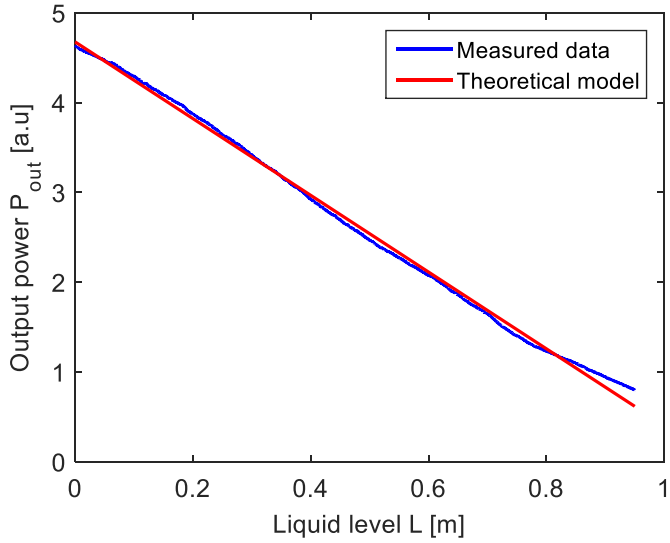

Fig. 9. Co-propagation configuration: Comparison between experimental and theoretical results.

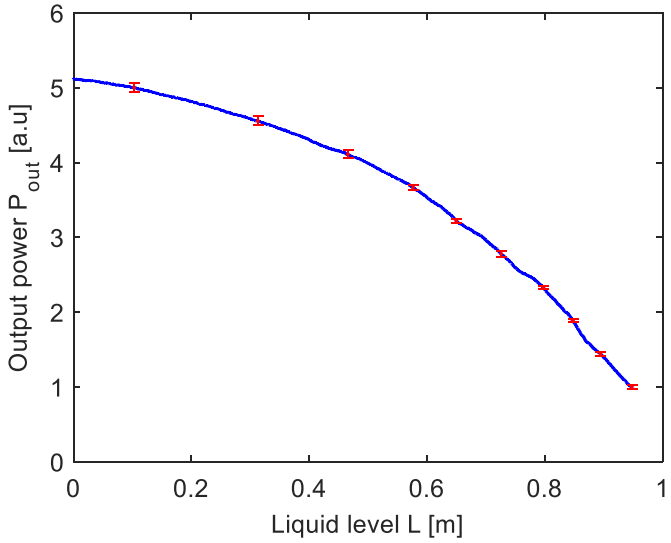

Fig. 11. Counter-propagation configuration: Average sensor response as a function of the liquid level; Error bars are also depicted.

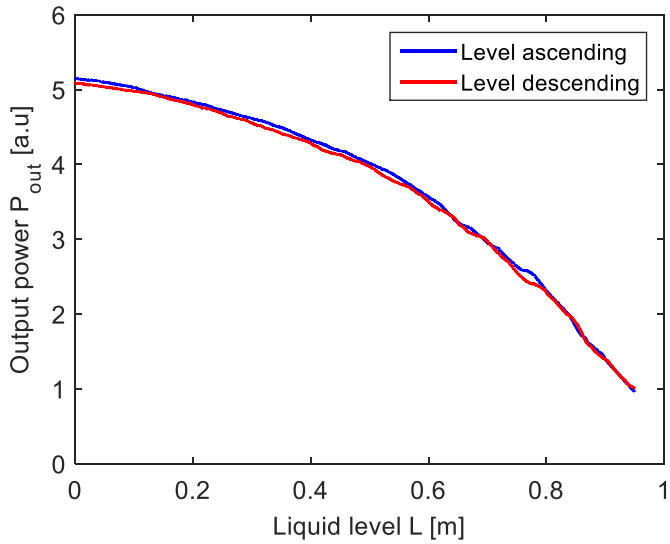

Fig. 10. Counter-propagation configuration: Sensor response as a function of the liquid level, for both increasing and decreasing liquid levels, from 0 to 950 mm.

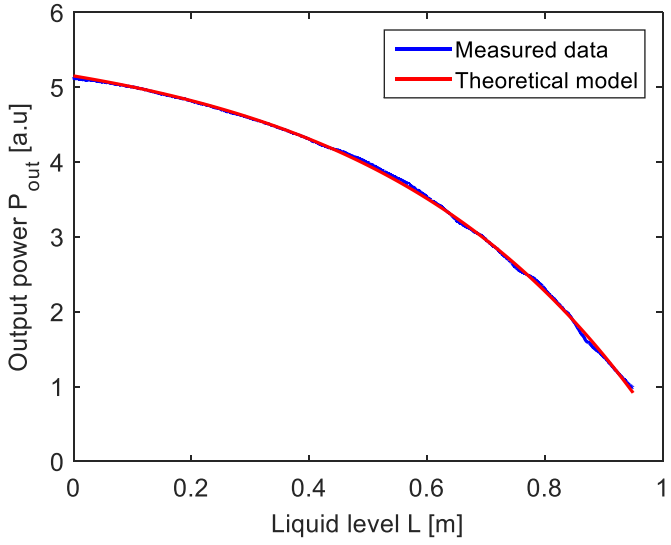

Fig. 12. Counter-propagation configuration: Comparison between experimental and theoretical results.

It can be observed that the sensor response with the decreasing level is almost equal to that with the increasing level. The average sensors response including the error bars is depicted in Fig. 8. The estimated sensitivity [32] is S ≈ -43fW/mm. The resolution ranges from $\pm$8mm at low liquid level up to $\pm$2mm at high liquid level [22]. The decrease of the resolution is related to the observed increase in measurement error as the coupling length increase.

The comparison of measured data with the results obtained via the theoretical model developed in Sect. II [see eq. (4)] is illustrated in Fig. 9. As it can be observed, the experimental data are well described by the analytical model. The quality of fit of the model has been determined by the coefficient of determination R^2, which has been found to be 0.9973, thus indicating that 99.73% of the variability in the response could be explained by the model.

B. Counter-Propagation Configuration

The tests have been repeated for the counter-propagation configuration. The liquid level response is shown in Fig. 10. When the liquid level changes from 0 to 950 mm, the output power decreases non-linearly. Also in this case there is a good agreement between the decreasing-level response and the increasing-level one. The average sensor response including error bars is depicted in Fig. 11. The resolution ranges from $\pm$30mm at low liquid level up to $\pm$1 mm at high liquid level. Also in this case the resolution decreases as the coupling length increases. The difference in the sensors resolution are related to

the nonlinear response of the sensor that exhibits a sensitivity that increase from S ≈ -20 fW/mm, at low liquid level, up to S ≈ -110 fW/mm at high liquid level. The comparison of measured data with the theoretical model developed in Section II is illustrated in Fig. 12. It is seen that the experimental data are well fitted by the analytical model [see eq. (7)]. The quality of fit of the model expressed by the coefficient of determination R^2 is 0.9997. Moreover, the estimated attenuation and coupling coefficient resulting from the fitting are $\alpha = 1.12\text{m}^{-1}$ and $\beta = 0.0084\ \text{m}^{-1}$, respectively. They are in good agreement with the measured and expected values.

VI. Conclusion

A fiber optic sensor able to measure continuously the liquid level inside a container has been proposed. The sensor is based on two parallel side diffusing optical fibers coupled together.

By setting a working wavelength that is strongly absorbed by the liquid, the power coupled between the fibers depends on the liquid level. The coupling between co-propagating and counter-propagating waves has been theoretically modelled and experimentally evaluated. Measurements results are in good agreement with the model results, thus showing that both configurations could be used for liquid level sensing. Co-propagation coupling configuration, however, exhibits a linear sensor response, while the counter-propagation configuration response is nonlinear. Accordingly, the former configuration offers a certain advantage in term of calibration procedure compared to the latter. In the co-propagation configurations the resolution ranges from $\pm$ 8mm at low liquid level up to $\pm$ 2mm at high liquid level over a wide measurement range ($\approx$1m). These results are comparable with the performances of interferometric sensors reported in table I, but avoiding the need of complex interrogation system or expensive detection instrumentation. With respect to intensity-modulated fiber optic level sensors developed in literature, like those based on side coupling, the resolution is lower [21]. However, by changing the probe geometry from a straight fiber configuration to a spiral configuration, in which the two fibers are wrapped around a supporting tube in a spiral shape, it is possible to increase the coupling fiber length per unit liquid level with an improvement of the performances [33]. Furthermore, the proposed approach does not require particular mechanical assembly procedure like bending, twisting or mechanical polishing of the fiber in order to induce the side coupling. The unique optical properties of side diffusing optical fibers permit an optical coupling also when the fiber are at a relatively large distance in terms of wavelength ($d \gg \lambda$). This approach strongly simplifies the probe manufacturing process and increases the overall robustness of the sensor.

In conclusion, the sensing properties of side diffusing optical fibers has been demonstrated for liquid level monitoring for the first time. The results obtained are promising and the work is ongoing to fully exploit the potential of the proposed approach. In particular, there are some questions that will be addressed in order to improve the performances, such as the theoretical modelling of coupling process, the optimization of sensor parameters and the enhancements of the probe geometry.

Acknowledgment

The authors would like to thank Mario Paniccia and Versalume for providing LDF samples and technical discussions.

References

[1] K. Loizou and E. Koutroulis, "Water level sensing: State of the art review and performance evaluation of a low-cost measurement system," *Measurement*, vol. 89, pp. 204–214, 2016.
[2] H. Zhang, Y. Wang, X. Zhang, D. Wang, and B. Jin, "Design and performance analysis of an intrinsically safe ultrasonic ranging sensor," *Sensors*, vol. 16, p. 867, 2016.
[3] K. P. Chen, B. McMillen, M. Buric, C. Jewart, and W. Xu, "Self-heated fiber Bragg grating sensors," *Appl. Phys. Lett.*, vol. 86, no. 14, 2005, Art. no. 143502.
[4] J. N. Wang and J. L. Tang, "Feasibility of fiber Bragg grating and long-period fiber grating sensors under different environmental conditions," *Sensors*, vol. 10, pp. 10105–10127, 2010.
[5] P. Raatikainen, I. Kassamakov, R. Kakanakov, and M. Luukkala, "Fiber-optic liquid-level sensor," *Sensors Actuators A*, vol. 58, pp. 93–97, 1997.
[6] G. Onorato, G. Persichetti, I. A. Grimaldi, G. Testa, and R. Bernini, "Optical fiber fuel level sensor for aeronautical applications," *Sensors Actuators A*, vol. 260, pp. 1–9, 2017.
[7] A. Wang, M. F Gunther, K. A Murphy, and R. O. Claus, "Fiber-optic liquid-level sensor," *Sensors Actuators A*, vol. 35, pp. 161–164, 1992.
[8] I. K. Ilev and R. W. Waynant, "All-fiber-optic sensor for liquid level measurement," *Rev. Sci. Instrum.*, vol. 70, pp. 2551–2554, 1999.
[9] P. Nath, P. Datta, and K. C. Sarma, "All fiber-optic sensor for liquid level measurement," *Microw. Opt. Technol. Lett.*, vol. 50, pp. 1982–1984, 2008.
[10] B. Yun, N. Chen, and Y. Cui, "Highly sensitive liquid-level sensor based on etched fiber Bragg grating," *IEEE Photon. Technol. Lett.*, vol. 19, pp. 1747–1749, 2007.
[11] H. Fu *et al.*, "Implementation and characterization of liquid-level sensor based on a long-period fiber grating Mach–Zehnder interferometer," *IEEE Sensors J.*, vol. 11, pp. 2878–2882, 2011.
[12] J. E. Antonio-Lopez, D. A. May-Arrioja, and P. LiKamWa, "Fiber-optic liquid level sensor," *IEEE Phot. Techn. Lett.*, vol. 23, pp. 1826–1828, 2011.
[13] C. Li *et al.*, "Liquid level measurement based on a no-core fiber with temperature compensation using a fiber Bragg grating," *Sensors Actuators A: Physical*, vol. 245, pp. 49–53, 2016.
[14] C. Li *et al.*, "Liquid level and temperature sensor based on an asymmetrical fiber Mach–Zehnder interferometer combined with a fiber Bragg grating," *Opt. Commun.*, vol. 372, pp. 196–200, 2016.
[15] B. Preložnik, D. Gleich, and D. Donlagic, "All-fiber, thermo-optic liquid level sensor," *Opt. Express*, vol. 26, pp. 23518–23533, 2018.
[16] M. Lomer, A. Quintela, M. Lopez-Amo, J. Zubia, J. M. Lopez-Higuera, "A quasi-distributed level sensor based on a bent side-polished plastic optical fibre cable," *Meas. Sci. Technol.*, vol. 18, pp. 2261–2267, 2007.
[17] G. Betta, A. Pietrosanto, and A. Scaglione, "A digital liquid level transducer based on optical fiber," *IEEE Trans. Instrum. Meas.*, vol. 45, no. 2, pp. 551–555, Apr. 1996.
[18] S. M. Chandani and N. A. F. Jaeger, "Optical fiber-based liquid level sensor," *Opt. Eng.*, vol. 11, 2000, Art. no. 114401.
[19] 7.Y. L. Hou *et al.*, "Polymer optical fiber twisted macro-bend coupling system for liquid level detection," *Opt. Express*, vol. 22, 23231–23241, 2014.
[20] H. X. Zhang *et al.*, "Polymer optical fiber continuous liquid level sensor for dynamic measurement," *IEEE Sensors J.*, vol. 15, pp. 5238–5242, 2015.
[21] Y. Zhang *et al.*, "Enhancement of a continuous liquid level sensor based on a macro-bend polymer optical fiber coupler," *IEEE Photon. J.*, vol. 10, no. 1, Feb. 2018, Art. no. 6800806.
[22] S. Logunov, E. Fewkes, F. Shustack, and F. Wagner, "Light diffusing optical fiber for illumination," in *Proc. Renewable Energy Environ.; OSA Tech. Dig. (Online), Opt. Soc. Amer.*, Washington, DC, USA, 2013, Paper DT3E.4.
[23] W. S. Klubben *et al.*, "Novel light diffusing fiber for use in medical applications," in *Proc. SPIE 9702, Opt. Fibers Sensors Medical Diagnostics Treatment Appl. XVI*, 2016, Art. no. 970218.
[24] D. Marcuse, *Theory of Dielectric Optical Waveguides*. 2nd Ed., New York, NY, USA: Academic, 1991.
[25] D. Marcuse, "Derivation of coupled power equations," *Bell Syst. Tech. J.*, vol. 51, pp. 229–237, 1972.
[26] H. E. Rowe, "Propagation in one-dimensional random media," *IEEE Trans. Microw. Theory Tech.*, vol. MTT-19, no. 1, pp. 73–80, Jan. 1971.

[27] D. Marcuse, "Coupled power equations for backward waves," *IEEE Trans. Microw. Theory Techn.*, vol. MTT-20, no. 8, pp. 541–546, Aug. 1972.
[28] M. Koshiba, K. Saitoh, K. Takenaga, and S. Matsuo, "Multi-core fiber design and analysis: Coupled-mode theory and coupled-power theory," *Opt. Express*, vol. 19, pp. B102–B111, 2011.
[29] Corning Fibrance light diffusing fiber, specification datasheet.
[30] S. Logunov, K. Bennett, E. Fewkes, S. Klubben, and M. Paniccia, "Silica nano-structured fiber for illumination," *J. Lightw. Technol.*, vol. 37, no. 22, pp. 5667–5673, Nov. 15, 2019.
[31] S. Kedenburg, M. Vieweg, T. Gissibl, and H. Giessen, "Linear refractive index and absorption measurements of nonlinear optical liquids in the visible and near-infrared spectral region," *Opt. Mater. Express*, vol. 2, pp. 1588–1611, 2012.
[32] J. L. Santos and F. Farahi, *Handbook of Optical Sensors*. Boca Raton, FL, USA: CRC Press, 2014.
[33] Y. Zhang *et al.*, "An optical fiber liquid level sensor based on side coupling induction technology," *J. Sens.*, vol. 2018, 2018, Art. no. 2953807.

Pasquale Imperatore received the *Laurea* degree *(summa cum laude)* in electronic engineering and the Ph.D. degree in electronic and telecommunication engineering, from the University of Naples Federico II. He is a Researcher with the Institute of electromagnetic sensing of the environment (IREA), Italian National Council of Research (CNR), Naples, Italy. He has more than 15 years of research experience in electromagnetic scattering and remote sensing. His research interests include theoretical scattering models, random layered media, SAR data modeling and processing, SAR interferometry, parallel algorithms for parallel/distributed computing environments and high-performance scientific applications. He acts as a reviewer for several peer-reviewed journals. Moreover, he has coedited two books in the field of remote sensing and geospatial technology.

Gianluca Persichetti He received the *Laurea* degree from the University of Naples Federico II, Naples, Italy, in 2003 and the Ph.D. degree in "Novel Technologies for Materials Sensors and Imaging" in 2010 at the same University.

He is currently a Researcher with the Institute for Electromagnetic Sensing of the Environment (IREA) of the National Research Council of Italy (CNR). His main research activities are the development of fiber optic sensors and spectroscopic sensors based on optofluidic waveguides.

Genni Testa received the Laurea degree *(summa cum laude)* in solid states physics from the University of Naples Federico II, Naples, Italy, in 2005, and the Ph.D. degree in electrical engineering from the Second University of Naples, Aversa, Italy, in 2008.

She is currently a Researcher with the Institute for the Electromagnetic Sensing of the Environment (IREA), Italian National Research council (CNR). Her research activities deal with the design, fabrication and characterization of microfluidic and optofluidic devices for biosensing and environmental applications. She is author or coauthor of more than 25 international journal papers and acts as a reviewer of several international journals.

Romeo Bernini received the *Laurea* degree *(summa cum laude)* from the University of Naples Federico II, Naples, Italy, and the Ph.D. degree from the Second University of Naples, Aversa, Italy, in electronic engineering, in 1995 and 1999, respectively.

He was a Research Fellow with the Second University of Naples, in 2000. He is currently a Senior Researcher with the Institute for the Electromagnetic Sensing of the Environment (IREA), Italian National Research council (CNR). His research fields are optoelectronic devices and sensors, microfluidic and optofluidic devices and fiber optic sensors. He has authored or coauthored more than 90 papers published in various international journals. He is a reviewer for several technical journals. He holds one international and two national patents on fiber optic sensors.